

University of Dundee

## **Aerobic and anaerobic biosynthesis of nano-selenium for remediation of mercury contaminated soil**

Wang, Xiaonan; Zhang, Daoyong; Pan, Xiangliang; Lee, Duu Jong; Al-Misned, Fahad A.; Mortuza, M. Golam

*Published in:*  
Chemosphere

*DOI:*  
[10.1016/j.chemosphere.2016.12.020](https://doi.org/10.1016/j.chemosphere.2016.12.020)

*Publication date:*  
2017

*Licence:*  
CC BY-NC-ND

*Document Version*  
Peer reviewed version

[Link to publication in Discovery Research Portal](#)

### *Citation for published version (APA):*

Wang, X., Zhang, D., Pan, X., Lee, D. J., Al-Misned, F. A., Mortuza, M. G., & Gadd, G. M. (2017). Aerobic and anaerobic biosynthesis of nano-selenium for remediation of mercury contaminated soil. *Chemosphere*, 170, 266-273. <https://doi.org/10.1016/j.chemosphere.2016.12.020>

### **General rights**

Copyright and moral rights for the publications made accessible in Discovery Research Portal are retained by the authors and/or other copyright owners and it is a condition of accessing publications that users recognise and abide by the legal requirements associated with these rights.

- Users may download and print one copy of any publication from Discovery Research Portal for the purpose of private study or research.
- You may not further distribute the material or use it for any profit-making activity or commercial gain.
- You may freely distribute the URL identifying the publication in the public portal.

### **Take down policy**

If you believe that this document breaches copyright please contact us providing details, and we will remove access to the work immediately and investigate your claim.

**Aerobic and anaerobic biosynthesis of nano-selenium for remediation of mercury  
contaminated soil**

Xiaonan Wang <sup>a, c</sup>, Geoffrey Michael Gadd <sup>a, d</sup>, Daoyong Zhang <sup>a, e</sup>, Xiangliang Pan <sup>a, b, \*</sup>, Duu-Jong  
Lee <sup>f</sup>, Fahad A. Al-Misned <sup>g</sup>, M. Golam Mortuza <sup>g, h</sup>

<sup>a</sup> *Xinjiang Key Laboratory of Environmental Pollution and Bioremediation, Xinjiang Institute of  
Ecology and Geography, Chinese Academy of Sciences, Urumqi 830011, China*

<sup>b</sup> *College of Environment, Zhejiang University of Technology, Hangzhou 310014, China*

<sup>c</sup> *University of Chinese Academy of Sciences, Beijing 100049, China*

<sup>d</sup> *Geomicrobiology Group, School of Life Sciences, University of Dundee, Dundee DD1 5EH,  
Scotland, UK*

<sup>e</sup> *State Key Laboratory of Environmental Geochemistry, Institute of Geochemistry, Chinese  
Academy of Sciences, Guiyang, 550002, China*

<sup>f</sup> *Department of Chemical Engineering, National Taiwan University, Taipei 10617, Taiwan*

<sup>g</sup> *Department of Zoology, College of Science, King Saud University, Riyadh 11451, Saudi Arabia*

<sup>h</sup> *Department of Zoology, Faculty of Life and Earth Science, Rajshahi University, Rajshahi 6205,  
Bangladesh*

\*For correspondence. E-mail [xiangliangpan@163.com](mailto:xiangliangpan@163.com) ; Tel. +86 991 7885 446; Fax +86 991  
7885 446.

© 2016. This manuscript version is made available under the CC-BY-NC-ND 4.0 license  
<http://creativecommons.org/licenses/by-nc-nd/4.0/>

26 **Running title:** Biosynthesis of nano-Se<sup>0</sup> and mercury remediation

27

## ABSTRACT

Selenium (Se) nanoparticles are often synthesized by anaerobes. However, anaerobic bacteria cannot be directly applied for bioremediation of contaminated top soil which is generally aerobic. In this study, a selenite-reducing bacterium, *Citrobacter freundii* Y9, demonstrated high selenite reducing power and produced elemental nano-selenium nanoparticles (nano-Se<sup>0</sup>) under both aerobic and anaerobic conditions. The biogenic nano-Se<sup>0</sup> converted 45.8-57.1% and 39.1-48.6% of elemental mercury (Hg<sup>0</sup>) in the contaminated soil to insoluble mercuric selenide (HgSe) under anaerobic and aerobic conditions, respectively. Addition of sodium dodecyl sulfonate enhanced Hg<sup>0</sup> remediation, probably owing to the release of intracellular nano-Se<sup>0</sup> from the bacterial cells for Hg fixation. The reaction product after remediation was identified as non-reactive HgSe that was formed by amalgamation of nano-Se<sup>0</sup> and Hg<sup>0</sup>. Biosynthesis of nano-Se<sup>0</sup> both aerobically and anaerobically therefore provides a versatile and cost-effective remediation approach for Hg<sup>0</sup>-contaminated surface and subsurface soils, where the redox potential often changes dramatically.

**Keywords:** Bioremediation; selenium; mercury; metal immobilization; selenium nanoparticles

## 1. Introduction

Mercury (Hg) is a naturally occurring non-essential highly toxic metal in the Earth's crust, and it is widely used in many industries such as the extraction of gold from ores, production of NaOH and chlorine in the chlor-alkali industry, and manufacture of compact fluorescent lamps, cosmetics, insecticides and herbicides (Boening, 2000). In some cases, improper use has led to extensive mercury pollution of soil. For example, mercury concentrations in the soil around a chlor-alkali plant in the Netherlands reached up to 1150 mg kg<sup>-1</sup> (Bernaus et al., 2006). Mercury emissions were also detected in surrounding soils and sealed waste ponds near a chlor-alkali factory (Southworth et al., 2004).

Mercury speciation in contaminated soil can be classified into water soluble, elemental, exchangeable, strongly-bound, organic, sulfide and residual fractions. Normally, elemental mercury comprises a small proportion of the total mercury in soil whereas in mercury or gold mining regions and in chlor-alkali plant soil, elemental mercury may account for a much larger part of the total mercury. In the Idrija mercury mine region, Slovenia, HgS is the predominant mercury fraction, followed by Hg<sup>0</sup> (Kocman et al., 2004). Elemental mercury accounted for ~95% of the total mercury in soils heavily contaminated with mercury in Venezuela (García-Sánchez et al., 2006). Soil beneath and adjacent to the Pavlodar Chemical Plant in Kazakhstan was also contaminated by mercury, and ~88-98% of the total mercury can be present as elemental mercury (Neculita et al., 2005). Therefore, there is an urgent need to treat

69 elemental mercury-contaminated soil, particularly that caused by the industries  
70 mentioned above.

71  
72 Selenium (Se) is in the same group as sulfur in the Periodic Table, and has an  
73 extremely high affinity for mercury with  $\Delta G^0 = -38.1 \text{ kJ mol}^{-1}$ , which is higher than  
74 that for sulfur (Ho et al., 2015). A large amount of work has been carried out on  
75 detection of mercury and selenium in fish, marine mammals and humans. The molar  
76 ratio of mercury to selenium in such samples was approximately 1, which suggested  
77 detoxification of mercury into less toxic mercuric selenide (HgSe) (Southworth et al.,  
78 2000; Squadrone et al., 2015). Selenium nanoparticles have already been shown to be  
79 effective for mercury removal from off gases, and unstabilized amorphous nano-Se<sup>0</sup>  
80 showed a strong mercury capture capacity of 188 mg g<sup>-1</sup> dry weight (Johnson et al.,  
81 2008; Lee et al., 2009). Biogenic red amorphous nano-Se<sup>0</sup> has also been applied to  
82 sequester mercury vapour released from mercury-contaminated museum specimens,  
83 the historic mercuric chloride treatment to preserve specimens leading to mercury  
84 volatilization (Fellowes et al., 2011). Nano-Se<sup>0</sup> therefore appears to be a promising  
85 mercury-trapping agent for cleanup, disposal, recycling and packaging applications  
86 (Ralston, 2008).

87  
88 Most of these examples of mercury removal by selenium are concerned with mercury  
89 vapour in the atmosphere. However, this technique can also be applied to the aquatic  
90 environment. For example, *Pseudomonas fluorescens* could reduce SeO<sub>3</sub><sup>2-</sup> and Hg<sup>2+</sup>

into elemental forms, the interaction between these two elements resulting in the formation of Hg-Se complexes within the cells with a Hg:Se molar ratio close to 1 (Yang et al., 2011). Bio-reduced  $\text{Hg}^0$  by a strain of *Shewanella putrefaciens* was captured as HgSe by extracellular biogenic amorphous selenium nanospheres (Jiang et al., 2012). However, no studies have been carried out which have tested the capacity of biogenic nano- $\text{Se}^0$  to immobilize mercury in soil.

Bioremediation of contaminated soil can be limited by the redox potential and the performance of the remediating bacteria in aerobic and anaerobic conditions. Surface soil layers are usually aerobic while subsurface soil layers may be anoxic, which means that both aerobic and anaerobic processes may be required. In addition, the soil redox potential during bioremediation may change drastically as bacterial cultures and substrates are applied. This may increase the cost, complexity and performance of bioremediation. Therefore, an ability for microbes to produce nano- $\text{Se}^0$  both aerobically and anaerobically may be relevant for the bioremediation of mercury-contaminated soils. Using versatile facultative bacteria to remediate soils with quite different redox potentials could be simpler and more effective.

In the present study, the performance of the facultative anaerobe *Citrobacter freundii* Y9, which can produce amorphous nano- $\text{Se}^0$  under anaerobic and aerobic conditions, in sequestering elemental mercury in soil was evaluated. Sequential soil extraction of mercury was carried out to determine changes in mercury speciation, and the reaction

113 products were characterized by scanning electron microscopy with energy-dispersive  
114 X-ray spectrometry (SEM-EDS), X-ray diffraction (XRD), transmission electron  
115 microscopy (TEM) and X-ray photoelectron spectroscopy (XPS).

116



## 2. Materials and methods

### 2.1. Bacteriogenic nano-Se<sup>0</sup>

*Citrobacter freundii* Y9, isolated from sludge from an anaerobic sulfate-reducing bioreactor in Urumqi, China was used in this study, and the sequence has been submitted to Gene Bank (number KF781347). The growth medium contained the following components: 1.0 g K<sub>2</sub>HPO<sub>4</sub>, 0.1 g MgCl<sub>2</sub>, 0.2% yeast extract, 10 mM sodium citrate in 1 L Milli-Q water. The medium was adjusted to pH 7.0-7.2 using 0.1 M HCl, and sterilized in a vertical heating pressure steam (LDZX-75KBS, Shanghai, China). The bacteria were cultured at 26<sup>0</sup>C in 500 ml serum bottles in a Whitley DG250 anaerobic workstation (Don Whitley Scientific, West Yorkshire, England), and aerobically in 250 ml flasks with constant shaking at 150 rpm.

To measure the selenite reduction activity of *C. freundii* Y9, late logarithmic phase cells (5%) were inoculated into fresh medium containing 1 mM sodium selenite, added from a sterile 500 mM sodium selenite stock solution. At appropriate time intervals, samples were collected and filtered using 0.22 µm hydrophilic polyestersulfone membranes. Selenite in the filtrates was analyzed by LC-HGAFS (Liquid Chromatography-Hydride Generation Atomic Fluorescence Spectrometry) (Jitian, Beijing, China). Determination of the number of viable cells (colony-forming units, CFU) was conducted as follows to measure the growth of bacteria (Tugarova et al, 2014). A series of consecutive ten-fold dilutions of bacterial suspensions were made using sterile physiological saline (0.87% NaCl); 200 µl of the corresponding

diluted samples were then spread on solid **nutrient broth medium** and cultured for 4-5 d at 26°C. Abiotic nano-Se<sup>0</sup> was prepared using L-ascorbic acid as a reductant to reduce H<sub>2</sub>SeO<sub>3</sub>, **polyvinyl alcohol (PVA, 0.05%)** was used as a soft template. The abiotic nano-Se<sup>0</sup> was centrifuged at 10,000×g for 10 min and then re-suspended in PVA solution (0.05%). Biogenic and abiotic selenium were characterized by SEM-EDS and XRD.

## *2.2. Elemental mercury immobilization in soil*

Biogenic and abiotic nano-Se<sup>0</sup> were used to capture mercury in contaminated soil under aerobic and anaerobic conditions. Soil was collected from farmland near Urumqi, China, sterilized in a vertical heating pressure steam (LDZX-75KBS, Shanghai, China), and air-dried, sieved (1 mm), and sterilized again under UV light irradiation for 2 h. **Liquid mercury was** added to the soil directly which was then aged for two months. The mercury immobilization tests were performed in centrifuge tubes which contained 25 g of elemental mercury contaminated soil and 25 ml medium containing 4 mM elemental selenium. When biogenic nano-Se<sup>0</sup> was used to treat mercury contaminated soil, one group contained 1% sodium dodecyl sulfate (SDS) to lyse the bacteria and release intracellular Se<sup>0</sup>. The original concentration of soil mercury was analyzed using a mercury analyzer (Lumex RP91C, Saint Petersburg, Russia). After one week, the different mercury fractions in the soil samples were analyzed. A control without addition of nano-Se<sup>0</sup> was also treated in the same way. The elemental selenium in the medium or in the **PVA** suspensions was centrifuged at

12,000×g for 10 min and then the Se-free supernatant was added to the control.

Anaerobic and aerobic immobilization were performed inside a Whitley DG250 anaerobic workstation or in a fume hood, respectively.

Sequential extraction procedures were used to evaluate mercury speciation in the soil, according to previously published methods (Biester and Scholz, 1996; Shi et al., 2005). Mercury compounds were classified into the following fractions: F1: total mercury; F2: elemental mercury; F3: water-soluble and exchangeable mercury; F4: mercury bound to organic matter; and F5: residual mercury. Total mercury (F1) was analyzed using a mercury analyzer (Lumex RP91C, Saint Petersburg, Russia) and this value was labelled THg1. For elemental mercury (F2), the soil was heated at 180°C for 2 h in a muffle furnace to separate out the elemental mercury. After this treatment, the total mercury left in the soil was again analyzed and this value was labelled THg2. The remaining soil was set aside for the following treatment. For water-soluble mercury and exchangeable mercury (F3), 20 ml Milli-Q water (18 MΩcm<sup>-1</sup>) was added to 2 g soil from the F2 treatment and shaken for 2 h. The mixture was then centrifuged for 20 min at 12,000×g. Another 20 ml of 1 M CaCl<sub>2</sub> (pH=5) was added to the soil and shaken for 2 h. The mixture was then centrifuged for 20 min at 12,000×g, then air dried. The total mercury left in the soil was again analyzed and this value was labelled THg3. The remaining soil was set aside for the following treatment. For mercury bound to organic matter (F4), 20 ml of 0.2 M NaOH was added to the treated soil from F3 and shaken for 2 h. The mixture was centrifuged as described previously,

and then 20 ml  $\text{CH}_3\text{COOH}$  4% (v/v) was added to the soil and shaken for 2 h. The mixture was then centrifuged as previously described, air dried and the total mercury left in the soil analyzed as above, which was labelled THg4. According to the following formulae, the concentrations of the different mercury fractions in the soil were obtained:  $F1 = \text{THg1}$ ;  $F2 = \text{THg1} - \text{THg2}$ ;  $F3 = \text{THg2} - \text{THg3}$ ;  $F4 = \text{THg3} - \text{THg4}$ ;  $F5 = \text{THg4}$ .

### 2.3. SEM-EDS, XRD, TEM and XPS analyses

The synthesized selenium particles and the soil after the experiments were analyzed by SEM-EDS. These samples were first freeze-dried in a vacuum freeze dryer (Labconco, Kansas, USA) then coated with gold with a sputter coater (Emitech K575, Kent, UK). Samples were examined using a scanning electron microscope (Zeiss Super 55VP, Oberkochen, Germany). Elemental analysis was carried out using energy-dispersive X-ray spectrometry (Bruker XFlash 5010, Berlin, Germany).

Samples for XRD were first freeze-dried, and then XRD spectra were obtained using an X-ray diffractometer (Bruker D8, Karlsruhe, Germany) with a Cu anode (40 kV and 30 mA) and scanning from 5 to  $80^\circ 2\theta$ .

In order to further characterize biogenic selenium particles, TEM was conducted as follows (Zhang and Frankenberger, 2006). Cells were harvested by centrifugation ( $10,000 \times g$ , 10 min) and fixed with 2.5% para-formaldehyde + 2.5% glutaraldehyde

in 0.1 M cacodylate buffer (pH 7.2) and post-fixed with 1% OsO<sub>4</sub> + 0.15% ruthenium red in 0.1 M cacodylate buffer. After washing three times with Milli-Q water, cells were dehydrated in graded acetone solutions (30, 50, 70, 90 and 100% for 15 min each time) and then embedded in Epon-Araldite. Blocks were sectioned using a Reichert Supernova Microtome (Leica AG, Wien, Austria) using a diamond knife producing sections approximately 80 nm in thickness. The samples were observed using a JEM-1200EX electron microscope (JEOL, Tokyo, Japan).

X-ray photoelectron spectroscopy was carried out on powders using a Thermo ESCALAB 250Xi spectrometer (Thermo Fisher Scientific, Waltham, MA, USA) using an Al Ka monochromatized source. Surface charging effects were corrected with a C 1s peak at 284.6 eV as a reference. Curve fitting and decomposition were achieved assuming Gaussian-Lorentzian fitting following Shirley background subtraction.

#### *2.4. Reagents*

All the chemicals and reagents used in this study were of analytical grade. **SDS**, H<sub>2</sub>SeO<sub>3</sub> and Na<sub>2</sub>SeO<sub>3</sub> were supplied by Guang Fu (Tianjin, China). Selenite was prepared as a 500 mM stock solution in Milli-Q water (18 MΩcm<sup>-1</sup>) and sterilized using 0.22 μm hydrophilic polyestersulfone membrane filters (Shanghai, China). Liquid mercury was obtained from Sinopharm Chemical Reagent (Shanghai, China). **PVA** was obtained from Sigma-Aldrich Ltd. L-ascorbic acid was supplied by Yong

227 Sheng (Tianjin, China).

228

## 229 *2.5. Statistical analysis*

230 The size of selenium particles was calculated using Image-Pro Plus 6.0 based on SEM

231 spectra. All experiments were carried out in triplicate; error bars on figures show

232 standard deviations'.

233

### 3. Results and discussion

#### 3.1. Bacteriogenic nano-Se<sup>0</sup>

*C. freundii* Y9 could reduce selenite to elemental selenium particles, which was evident by the colour of the medium changing to red/orange, under both aerobic and anaerobic treatments. There was no colour change and no change of selenite concentration in the abiotic control which demonstrated that it was the presence of growing bacteria that led to the reduction of selenite. After inoculation, bacterial growth was concomitant with the process of reduction. *C. freundii* Y9 showed more tolerance to selenite under anaerobic conditions and over 24 h, the medium turned red, and there was a rapid decrease in selenite concentration with complete removal after 5 d (Fig. 1). However, under aerobic conditions the medium turned a weaker red after 24 h with the efficiency of selenite reduction being 27% after 5 d incubation, the concentration of selenite remaining stable after this time (Fig. 1). Anaerobic selenite reduction was rapid and more pronounced than in aerobic conditions. In an anaerobic mode of respiration, selenite can be used as an electron acceptor in dissimilatory reduction (Macy et al., 1989), or be reduced and incorporated into organic compounds in assimilatory reduction (Lortie et al., 1992; Gadd, 1993). However, the mechanisms under aerobic conditions are not clearly understood.

SEM of *C. freundii* Y9 showed that particles were present inside the cells after exposure to 1 mM selenite; such particles were also detected extracellularly (Fig. 2b, c, d). EDS spectra of the particles confirmed the presence of selenium with characteristic

selenium absorption peaks at 1.37 and 11.22 keV (Fig. 2e). The calculated diameter of selenium particles ranged from 200-800 nm, with the average diameter being  $580 \pm 109$  nm. XRD patterns showed a broad peak at  $2\theta$  values from  $25^\circ$  to  $30^\circ$ , which indicated that the selenium particles formed were amorphous in nature (Fig. 2f). TEM showed that electron-dense particles were present inside the cells near the cytoplasmic membrane after incubation with 1 mM selenite (Fig. 2g, h). The biogenic selenium was deposited inside the cells or extracellularly and during cell lysis the elemental selenium could be released into the extracellular medium.

*C. freundii* is commonly found in soil, freshwater and marine habitats. Although, selenate reduction has been reported in *C. freundii* (Zhang et al., 2008), there is less work on selenite reduction, and the electron transfer system is different between selenate and selenite reduction in this organism (Siddique et al., 2006). As selenate is generally more toxic than selenite (Hockin and Gadd, 2003, 2006), it is perhaps better to use selenite as an electron acceptor to obtain nano- $\text{Se}^0$ .

### 3.2. Abiotic nano- $\text{Se}^0$

The mixture of PVA-stabilized selenium nanoparticles had a red/orange colour and remained stable on prolonged incubation. SEM and EDS spectra confirmed the presence of elemental nano- $\text{Se}^0$  (Fig. 3). The diameters of these nano- $\text{Se}^0$  particles ranged from 10-90 nm with an average value of  $71 \pm 16$  nm. However, without PVA in solution, a dark red precipitate of  $\text{Se}^0$  appeared. The XRD pattern of



chemically-reduced elemental selenium was the same as that for biogenic elemental selenium, indicating that the elemental selenium formed here was also amorphous.

### *3.3. Elemental mercury immobilization in soil*

The ability of biogenic and abiotic elemental amorphous nano-Se<sup>0</sup> to immobilize Hg<sup>0</sup> in soil was comparatively studied. The total mercury in the contaminated soil was  $21.43 \pm 2.51 \mu\text{g g dry weight}^{-1}$  which is ~350-fold higher than values commonly found. Elemental mercury was the primary fraction ( $17.63 \pm 2.10 \mu\text{g g}^{-1}$  dry weight) which accounted for 78.2-84.6% of the total mercury, while 11.1-11.7% ( $2.46 \pm 0.28 \mu\text{g g}^{-1}$ ) of the mercury occurred in the insoluble residual mercury fraction. When mercury-contaminated soil was supplied with nano-Se<sup>0</sup>, the total mercury decreased only slightly, some possibly being volatilized or adhering to surfaces of the bioreactor. However, the mercury speciation changed significantly, especially in the elemental and residual fractions (Fig. 4). Under anaerobic conditions, Hg<sup>0</sup> present in the mercury-contaminated control decreased by 11.3% ( $1.99 \mu\text{g g}^{-1}$ ). However, there was a 73.5% ( $12.96 \mu\text{g g}^{-1}$ ) and 63.5% ( $11.20 \mu\text{g g}^{-1}$ ) decrease in Hg<sup>0</sup> when the soil was supplied with biogenic Se<sup>0</sup> + SDS and biogenic Se<sup>0</sup>, respectively. The SDS was used in an attempt to release intracellular Se<sup>0</sup> from the bacterial cells and therefore enhance the reaction between Hg<sup>0</sup> and Se<sup>0</sup>. For the abiotic Se<sup>0</sup> treatment, 49.2% ( $8.68 \mu\text{g g}^{-1}$ ) of the Hg<sup>0</sup> fraction decreased. Under aerobic conditions, Hg<sup>0</sup> present in the control decreased by 12.5% ( $2.67 \mu\text{g g}^{-1}$ ). However, there was a 65.8% ( $11.60 \mu\text{g g}^{-1}$ ) and 61.25% ( $10.79 \mu\text{g g}^{-1}$ ) decrease in Hg<sup>0</sup> when the soil was supplied with biogenic Se<sup>0</sup> +

300 SDS and biogenic  $\text{Se}^0$ , respectively. For the abiotic aerobic  $\text{Se}^0$  treatment,  $\text{Hg}^0$   
301 decreased by 38.9% ( $6.87 \mu\text{g g}^{-1}$ ). Concomitant with the decrease in  $\text{Hg}^0$ , the residual  
302 mercury fraction was found to increase significantly. Under anaerobic conditions,  
303 residual mercury in the mercury-contaminated control increased by  $0.73 \mu\text{g g}^{-1}$ .  
304 However, there was a  $10.79 \mu\text{g g}^{-1}$  and  $8.80 \mu\text{g g}^{-1}$  increase in residual mercury when  
305 the soil was supplied with biogenic  $\text{Se}^0 + \text{SDS}$  and biogenic  $\text{Se}^0$ , respectively. For the  
306 abiotic  $\text{Se}^0$  treatment, residual mercury increased by  $4.44 \mu\text{g g}^{-1}$ . Under aerobic  
307 conditions, residual mercury in the control increased by  $0.85 \mu\text{g g}^{-1}$ . However, there  
308 was a  $9.41 \mu\text{g g}^{-1}$  and  $7.75 \mu\text{g g}^{-1}$  increase in residual mercury when the soil was  
309 supplied with biogenic  $\text{Se}^0 + \text{SDS}$  and biogenic  $\text{Se}^0$ , respectively. For the abiotic  
310 aerobic  $\text{Se}^0$  treatment, residual mercury was increased by  $3.15 \mu\text{g g}^{-1}$ . Thus, addition  
311 of abiotic or bacterially-produced **nano- $\text{Se}^0$**  to mercury-contaminated soil under  
312 anaerobic and aerobic conditions led to a decrease in the proportion of  $\text{Hg}^0$  present,  
313 and an increase in the insoluble residual Hg fraction.

314  
315 The efficiency of abiotic **nano- $\text{Se}^0$**  preparations was less than that for biogenic  
316 **nano- $\text{Se}^0$**  after SDS treatment which is surprising since the diameter of the abiotic  
317 **nano- $\text{Se}^0$**  (10-90 nm) was much smaller than that of biogenic **nano- $\text{Se}^0$**  (200-800 nm).  
318 In general terms, selenium capture of mercury occurs by a gas-solid reaction where  
319 the capacities and kinetics mainly depend on surface area: smaller particles have a  
320 larger specific surface area (Johnson et al., 2008). However, the **PVA** template may  
321 have blocked some elemental mercury access to elemental selenium which would

inhibit the reaction between selenium and mercury. Other workers have found similar results, e.g. BSA-stabilized nano-Se<sup>0</sup> had a lower sorption capacity than conventional selenium powder despite a much smaller particle size (6-60 nm vs 10-200 μm) (Johnson et al., 2008). Thus, biogenic nano-Se<sup>0</sup> gave a better performance for Hg<sup>0</sup> immobilization in soil.

### *3.4 Speciation of Hg immobilized in soil*

According to the SEM-EDS of immobilization products (Fig. 5), the atomic ratio of Hg:Se is close to 1 (Table 1), which revealed the formation of HgSe. XRD (Fig. 6) also confirmed that mercury and selenium were in the form of HgSe (PDF#65-2892). XPS analysis shows that binding energy of Hg 4f<sub>7/2</sub> and Hg 4f<sub>5/2</sub> was observed at 99.2 eV and 104.3 eV, respectively (Fig. 7), indicating that mercury could be present as HgSe and HgO (Zylberajch-Antoine et al., 1991). Deconvolution of the high resolution XPS spectra of selenium shows the presence of binding energy peaks of Se 3d<sub>5/2</sub> at 53.8 eV and Se 3d<sub>3/2</sub> at 54.5 eV, which is in good agreement with that previously reported for HgSe (Wall et al., 1986). The binding energy values for Se<sup>0</sup> at Se 3d<sub>5/2</sub> (54.7 eV) and Se 3d<sub>3/2</sub> (55.2 eV) were in accordance with those reported in the literature (Miyake et al., 1984). The XPS results confirmed immobilization of Hg<sup>0</sup> by nano-Se<sup>0</sup> as HgSe.

To date, many technologies have been examined for remediation of mercury-contaminated soil, such as immobilization (stabilization or solidification)

electro-remediation, soil flushing and soil washing, vitrification, thermal desorption and phytoremediation (Wang et al., 2012). Thermal treatment is the most widely used method although the treated soil is unsuitable for reuse due to the destruction of original soil properties (Yang et al., 2008), with some techniques also leading to mercury release into the air (Wang et al., 2012). The work presented here has shown that **amorphous nano-Se<sup>0</sup>** is capable of capturing Hg<sup>0</sup> in both surface and subsurface soil, thereby reducing mobility due to the production of HgSe. HgS is the typical residual form of mercury in soil, but HgSe also has a very low solubility ( $K_{sp}=10^{-58}$ ) and is more stable than HgS (Björnberg et al., 1988). As well as this, the use of nano-Se<sup>0</sup> appears safer since HgSe is chemically inert and a much less toxic compound compared to other forms of mercury and selenium. In addition, nano-Se<sup>0</sup> is unharmed, and the median lethal dose (LD50) for nano-Se<sup>0</sup> is 6.7 g kg<sup>-1</sup> in rats (Cummins and Kimura, 1971). Therefore, immobilization of mercury with nano-Se<sup>0</sup> may provide an efficient means of soil remediation with no secondary pollution and no volatilization. **However, soil is a heterogeneous complex environment, and it is necessary to consider the wider applicability of this technique across different soil types and physico-chemical conditions as well as the stability of nano-Se<sup>0</sup>. Moreover, the effects of different soil compositions and conditions on the reaction between nano-Se<sup>0</sup> and Hg<sup>0</sup> also need to be taken into consideration.**

#### **4. Conclusions**

This work is the first demonstration that **amorphous nano-Se<sup>0</sup>** can be applied to

capture  $\text{Hg}^0$  in soil under both aerobic and anaerobic conditions. It is concluded that *C. freundii* could be more easily and successfully applied for remediation of surface and subsurface soils, where the redox potential often changes dramatically. The experiments have revealed the formation of non-reactive  $\text{HgSe}$  by amalgamation of elemental selenium and elemental mercury which provides a potential approach for mercury immobilization in mercury-contaminated sites.

### **Conflict of Interest**

The authors declare that they have no conflict of interest.

### **Acknowledgements**

This work was supported by the National Natural Science Foundation of China (U1120302 and 21177127). G. M. Gadd gratefully acknowledges receipt of an award under the Chinese Government's 1000 Talents Plan with the Xinjiang Institute of Ecology and Geography, Chinese Academy of Sciences, Urumqi, China. G. M. Gadd also gratefully acknowledges an award (NE/M01090/1) under the National Environmental Research Council (UK) Security of Supply of Mineral Resources Grant Program: Tellurium and Selenium Cycling and Supply (TeASe). Partial funding for this research was also received from the Visiting Professor Program at King Saud University, Riyadh, Saudi Arabia.

**References:**

- Bernaus, A., Gaona, X., Derk, V.R., Valiente, M., 2006. Determination of mercury in polluted soils surrounding a chlor-alkali plant: direct speciation by X-ray absorption spectroscopy techniques and preliminary geochemical characterisation of the area. *Anal. Chim. Acta* 565, 73-80.
- Biester, H., Scholz, C., 1996. Determination of mercury binding forms in contaminated soils: mercury pyrolysis versus sequential extractions. *Environ. Sci. Technol.* 31, 233-239.
- Björnberg, A., Håkanson, L., Lundbergh, K., 1988. A theory on the mechanisms regulating the bioavailability of mercury in natural waters. *Environ. Pollut.* 49, 53-61.
- Cummins, L.M., Kimura, E.T., 1971. Safety evaluation of selenium sulfide anti-dandruff shampoos. *Toxicol. Appl. Pharmacol.* 20, 89-96.
- Boening, D.W., 2000. Ecological effects, transport, and fate of mercury: a general review. *Chemosphere* 40, 1335-1351.
- Fellowes, J.W., Patrick, R.A., Green, D.I., Dent, A., Lloyd, J.R., Pearce, C.I., 2011. Use of biogenic and abiotic elemental selenium nanospheres to sequester elemental mercury released from mercury contaminated museum specimens. *J. Hazard. Mater.* 189, 660-669.
- Gadd, G.M., 1993. Microbial formation and transformation of organometallic and organometalloid compounds. *FEMS Microbiol. Rev.* 11, 297-316.
- García-Sánchez, A., Contreras, F., Adams, M., Santos, F., 2006. Atmospheric mercury emissions from polluted gold mining areas (Venezuela). *Environ. Geochem. Health* 28,

409 529-540.

410 Ho, C.T., Nguyen, A.T., Duong, T.T., Dang, D.K., Tang, T.C., Hur, H.G., 2015.

411 Biologically based method for the synthesis of Hg–Se nanostructures by *Shewanella*

412 spp. RSC Adv. 5, 20764-20768.

413 Hockin, S.L., Gadd, G.M., 2003. Linked redox precipitation of sulfur and selenium

414 under anaerobic conditions by sulfate-reducing bacterial biofilms. Appl. Environ.

415 Microbiol. 69, 7063-7072.

416 Hockin, S., Gadd, G.M., 2006. Removal of selenate from sulfate-containing media by

417 sulfate-reducing bacterial biofilms. Environ. Microbiol. 8, 816-826.

418 Jiang, S., Ho, C.T., Lee, J.H., Duong, H.V., Han, S., Hur, H.G., 2012. Mercury capture

419 into biogenic amorphous selenium nanospheres produced by mercury resistant

420 *Shewanella putrefaciens* 200. Chemosphere 87, 621-624.

421 Johnson, N.C., Manchester, S., Sarin, L., Gao, Y., Kulaots, I., Hurt, R.H., 2008.

422 Mercury vapor release from broken compact fluorescent lamps and in situ capture by

423 new nanomaterial sorbents. Environ. Sci. Technol. 42, 5772-5778.

424 Kocman, D., Horvat, M., Kotnik, J., 2004. Mercury fractionation in contaminated

425 soils from the Idrija mercury mine region. J. Environ. Monit. 6, 696-703.

426 Lee, B., Sarin, L., Johnson, N.C., Hurt, R.H., 2009. A nano-selenium reactive barrier

427 approach for managing mercury over the life-cycle of compact fluorescent lamps.

428 Environ. Sci. Technol. 43, 5915-5920.

429 Lortie, L., Gould, W.D., Rajan, S., McCready, R.G.L., Cheng, K.J., 1992. Reduction

430 of selenate and selenite to elemental selenium by a *Pseudomonas stutzeri* isolate. Appl.

431 Environ. Microbiol. 58, 4042-4044.

432 Macy, J.M., Michel, T.A., Kirsch, D.G., 1989. Selenate reduction by a *Pseudomonas*  
 433 species: a new mode of anaerobic respiration. FEMS Microbiol. Lett. 61, 195-198.

434 Miyake, I., Tanpo, T., Tatsuyama, C., 1984. XPS study on the oxidation of InSe. Jpn. J.  
 435 Appl. Phys. 23, 172.

436 Neculita, C.M., Zagury, G.J., Deschênes, L., 2005. Mercury speciation in highly  
 437 contaminated soils from chlor-alkali plants using chemical extractions. J. Environ.  
 438 Qual. 34, 255-262.

439 Ralston, N. Nano-selenium captures mercury. Nat. Nanotechnol. 2008; 3: 648.

440 Shi, J., Liang, L., Jiang, G., Jin, X., 2005. The speciation and bioavailability of  
 441 mercury in sediments of Haihe River, China. Environ. Int. 31, 357-365.

442 Siddique, T., Zhang, Y., Okeke, B.C., Frankenberger, W.T., 2006. Characterization of  
 443 sediment bacteria involved in selenium reduction. Bioresour. Technol. 97, 1041-1049.

444 Southworth, G.R., Lindberg, S.E., Zhang, H., Anscombe, F.R., 2004. Fugitive mercury  
 445 emissions from a chlor-alkali factory: sources and fluxes to the atmosphere. Atmos.  
 446 Environ. 38, 597-611.

447 Southworth, G.R., Peterson, M.J., Ryon, M.G., 2000. Long-term increased  
 448 bioaccumulation of mercury in largemouth bass follows reduction of waterborne  
 449 selenium. Chemosphere 41, 1101-1105.

450 Squadrone, S., Benedetto, A., Brizio, P., Prearo, M., Abete, M.C., 2015. Mercury and  
 451 selenium in European catfish (*Silurus glanis*) from Northern Italian Rivers: Can molar  
 452 ratio be a predictive factor for mercury toxicity in a top predator? Chemosphere 119,



453 24-30.

454 Tugarova, A.V., Vetchinkina, E.P., Loshchinina, E.A., Burov, A.M., Nikitina, V.E.,  
 455 Kamnev, A.A., 2014. Reduction of selenite by *Azospirillum brasilense* with the  
 456 formation of selenium nanoparticles. *Microb. Ecol.* 68, 495-503.

457 Wall, A., Caprile, C., Franciosi, A., Vaziri, M., Reifenberger, R., Furdyna, J., 1986.  
 458 Bonding and stability in narrow-gap ternary semiconductors for infrared applications.  
 459 *J. Vac. Sci. Technol. A* 4, 2010-2013.

460 Wang, J., Feng, X., Anderson, C.W., Xing, Y., Shang, L., 2012. Remediation of  
 461 mercury contaminated sites – a review. *J. Hazard. Mater.* 221, 1-18.

462 Yang, D., Chen, Y., Belzile, N., 2011. Evidences of non-reactive mercury-selenium  
 463 compounds generated from cultures of *Pseudomonas fluorescens*. *Sci. Total Environ.*  
 464 409, 1697-1703.

465 Yang, D., Chen, Y., Gunn, J.M., Belzile, N., 2008. Selenium and mercury in  
 466 organisms: interactions and mechanisms. *Environ. Rev.* 16, 71-92.

467 Zhang, Y., Frankenberger, W.T., 2006. Removal of selenite in river and drainage  
 468 waters by *Citrobacter braakii* enhanced with zero-valent iron. *J. Agric. Food Chem.*  
 469 54, 152-156.

470 Zhang, Y., Okeke, B.C., Frankenberger, W.T., 2008. Bacterial reduction of selenate to  
 471 elemental selenium utilizing molasses as a carbon source. *Bioresour. Technol.* 99,  
 472 1267-1273.

473 Zylberajch-Antoine, C., Barraud, A., Roulet, H., Dufour, G., 1991. XPS  
 474 characterization of inserted mercury sulfide single layers in a Langmuir-Blodgett

475 matrix. Appl. Surf. Sci. 52, 323-327.

476

**Table 1.** The atom concentrations of selenium, mercury and the atomic ratio between selenium and mercury in mercury-contaminated soil after addition of elemental selenium.

	1	2	3	4	5	6	7	8
Atom.C: Hg [at.%]	24.11	19.63	26.09	21.53	24.62	25.89	25.51	28.02
Atom.C: Se [at.%]	21.99	22.02	23.87	20.52	22.15	23.98	22.59	23.8
Atomic ratio Hg/Se	1.096	0.891	1.093	1.049	1.111	1.080	1.129	1.177

As shown in Fig. 5(a), eight points were selected for EDS, and the concentrations of selenium, mercury and the atomic ratio between selenium and mercury were calculated according to the EDS results.

## Figure legends

**Fig. 1.** Growth and reduction kinetics at an initial concentration of 1 mM Na<sub>2</sub>SeO<sub>3</sub>.

Symbols represent: (■) selenite concentration under anaerobic conditions; (□) selenite

concentration under aerobic conditions; (▼) CFU under a

CFU under aerobic conditions. Error bars (n=3) represent the standard deviation.

**Fig. 2.** Characterization of elemental selenium produced by *C. freundii* Y9. (a) SEM

micrographs of *C. freundii* Y9. (b, c, d) SEM micrographs of *C. freundii* Y9 grown in

the presence of 1 mM selenite for 5 d. (e) EDS spectrum and (f) XRD pattern of red

selenium particles produced by *C. freundii* Y9 grown in the presence of 1 mM selenite

for 5 d. (g, h) Transmission electron micrographs of the cells cultured in 1 mM


selenite for 5 d. Scale bars: (a, b) 1 μm; (c, d, g, h) 200 nm. Typical results are shown


from one of several determinations.

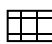
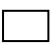
**Fig. 3.** SEM micrograph of abiotic elemental selenium. Scale bars = 1 μm. A typical

micrograph is shown from one of several determinations.

**Fig. 4.** Different fractions of mercury in soil before and after experimental treatments.

(a) anaerobic conditions. (b) aerobic conditions. Symbols represent:  total

mercury;  elemental mercury;  water soluble and exchangeable mercury;

 mercury bound to organic matter;  residual mercury. Error bars (n=3)

represent the standard deviations.

**Fig. 5.** SEM-EDS micrograph of mercury contaminated soil after addition of elemental selenium. (a) SEM micrograph (scale bar = 2  $\mu\text{m}$ ) and (b) EDS spectrum of mercury contaminated soil after addition of elemental selenium. Typical results are shown from one of several determinations.

**Fig. 6.** XRD pattern of mercury contaminated soil after addition of elemental selenium. (a) XRD pattern of mercury contaminated soil. (b) XRD pattern of mercury contaminated soil with addition of elemental selenium. A typical pattern is shown from one of two determinations both of which gave similar results.

**Fig.7.** High resolution XPS spectrum. (a) XPS spectroscopy of Hg 4f in experimental soil; (b) XPS spectroscopy of Se 3d in experimental soil. Symbols represent: ..... experimental spectrum; — interpolate spectrum; — fitted peaks; — loss feature; — background.